Revista Minelor – Mining Revue
ISSN-L 1220-2053 / ISSN 2247-8590
vol. 27, issue 3 / 2021, pp. 30-39

ENERGY ANALYSIS OF IMPACT-SHEAR INTERACTION OF COUNTER FLOWS OF GROUND LOOSE MATERIAL IN CENTRIFUGAL DISINTEGRATOR

Volodymyr NADUTYI[1], Oleksandr TYTOV[2], Dmytrii KOLOSOV[3], Vitalii SUKHARIEV[4], Taras USATYI[5]*

[1]Dnipro University of Technology, Dnipro, Ukraine, nadutyvp@gmail.com
[2]Dnipro University of Technology, Dnipro, Ukraine, tytov.o.o@nmu.one
[3]Dnipro University of Technology, Dnipro, Ukraine, evolyuta@gmail.com
[4]Dnipro University of Technology, Dnipro, Ukraine, agnivik@ukr.net
[5]Dnipro University of Technology, Dnipro, Ukraine, usatuits@gmail.com

DOI: 10.2478/minrv-2021-0023

Abstract: *The distribution of power consumption of centrifugal two-shaft disintegrator for impact and shear destruction of material as functions of its technological and structural parameters, as well as parameters of material being ground, has been substantiated. An analytical apparatus has been developed to determine the degree of influence of each factor. Factors affecting the absolute value of the consumed power of the disintegrator have also been established. The results of the work make it possible to optimize the technological process in order to reduce the yield of bream fragments of destruction, which is observed when the share of energy of shear deformations increases, in order to obtain cuboid fractions of disintegration products. They allow to create a methodology for determining the rational parameters of a centrifugal double-shaft disintegrator.*
Keywords: *centrifugal double-shaft disintegrator, counter flows, loose material, lamellar piece, impact, shift, power distribution*

1. Problem statement

Centrifugal type disintegrators are increasingly used for rock mass processing. They are usually distinguished by low specific metal consumption and low yield of lamellar pieces compared, for example, with traditional cone crushers [1]. An additional advantage is the ability to work with fine-grained materials to obtain a size of the final product less than a millimeter.

The effect of reducing the yield of lamellar pieces in disintegration product is achieved due to the free impact of initial piece on another piece or a rigid barrier. Here, the main cracks have the ability to spread from a single, as a rule, point of contact towards local weakening of the rock, for example, defects or cleavage planes of minerals [2].

Two fundamentally different types of structures can be distinguished for centrifugal disintegrators.

The first type is disintegrators with so-called "impact" rotor, which includes hammer and rotary crushers [3]. Quickly rotating working elements strike a fairly slow moving piece, its fragments acquire great kinetic energy and collide with baffle plates, then again with other working elements, and so several times in one pass. The greatest wear of metal occurs precisely when hitting a piece of rock, especially if this element is rigidly fixed. Therefore, rotary crushers are characterized by the greatest wear of working elements, which significantly affects operating costs and increases the time of repair breaks.

The second type includes disintegrators with an "acceleration" rotor, for example, of the Barmac type [3]. The initial material accelerates relatively smoothly inside the rotor, flies off it and collides with the self-lined covering body on the principle of "stone against stone." The greatest wear is observed for the acceleration blades located at the outlet of the material from the rotor, however, due to the use of self-lining both inside and outside the rotor, the wear is less than, for example, for rotary crushers.

[*] Corresponding author: Volodymyr Nadutyi, Prof. PhD. Eng., Dnipro University of Technology, Dnipro, Ukraine, contact details (Dnipro University of Technology, Dnipro, Ukraine, nadutyvp@gmail.com)

Regardless of disintegrator type, such a pattern is observed: the harder the rock, the higher the speed of pieces flying-off is required and the more the wear of working surfaces.

In two-shaft centrifugal disintegrators, the pieces' impact speed doubles, with other things being equal, due to the counter contact of the material flows from two different rotors placed in adjacent chambers [4]. The material flows are undergone both the loads from high-speed impact and the shear deformations at tangent contact of two flows. It reduces sharply a yield of lamellar particles. However, this type of disintegrators is rather new and demands a detailed research of disintegration process mechanics for the purpose of its efficiency management.

2. Analysis of recent research and publications

Today, there are more and more publications on the usefulness of using of the cuboid crushed stone having lamellar grains content not more than 10-15% instead of other groups of crushed stone in various industries using solid mineral raw materials.

The following data show the demand for cubic crushed stone, for example, in road construction. According to standard [5], the most preferred option for obtaining high-quality road surface is the use of crushed stone mixtures with a content of lamellar and needle particles of not more than 10% by weight with a maximum grain size of 5 mm, or not more than 15% with a maximum grain size in the range of 10-40 mm. At the same time, the yield of cuboid grains should be at least 50% of crushed stone mass for all indicated mixtures.

In the work [6], it is indicated the use of high-strength fine-grained concrete for the production of tiles. The use of fine aggregate gives the concrete the following properties:

- the water content reducing, the homogeneity and the resistance to stratification improving, the workability improving;
- the increase of concrete mixture thixotropy, which facilitates and accelerates the processes of its transportation, laying, compaction, improves the product surface quality;
- the acceleration of solidification rate;
- the possibility to eliminate the heat treatment of piece products;
- the significant improvement of mold properties of concrete mixtures.

The production of conditioned fine aggregate in conventional cone fine crushers is often impossible not only by the yield of lamellar grains, but also by the size of the product. Therefore, the emphasis in the studies is made on disintegrators with centrifugal and vibration force fields.

It is stated in work [7], that the production of cuboid crushed stone in traditional cone crushers is the most appropriate. They differ from centrifugal disintegrators with an acceleration rotor by the lower energy consumption and the yield of fines being the loss of crushed stone fractions of 5-20 mm during crushing. However, the metal consumption of cone inertial crushers is rated as "high," while centrifugal disintegrators have the same parameter as "low," two steps lower, which is the undeniable advantage of the latter.

The results of operation of DKD-300 six-rotor impact crusher are described in work [8]. It has been experimentally established, that large pieces are most intensively destroyed when crushing by free impact interaction. In addition, the supply of larger feed increases the yield of fine fractions, and vice versa.

The mathematical model presented in work [9] describes the movement of material pieces along the rough distribution disk in the loading zone of centrifugal impact crusher before coming into contact with acceleration blades. Here, the movement of the pieces without losing contact with the rough working surface under influence of centrifugal and Coriolis accelerations is considered.

Theoretical studies on simulation of collision of ellipsoidal particles in vibrational two-shaft centrifugal module [10] have shown, that during centrifugal disintegration with impact of opposite flows of particles of polydisperse composition, the particles of size less than the flow average value are most intensively destroyed. The collision of oncoming flows during disintegration of narrow fractions requires up to 20% less energy to achieve the same result of destruction compared to breaking by a rigid barrier.

3. The previously unresolved part of the general problem

Today, the field of single-shaft centrifugal disintegrators, especially with an impact rotor, is the most developed in theoretical terms. As for two-shaft machines, only the general aspects of impact of individual pieces and the experimental results of disintegration are considered. But there is almost completely no description of the interaction of counter material flows, which leads, besides, to the destruction of particles due to shear loadings. And it is precisely the determination of share of consumed energy, which is spent on more energy saving shear destruction of particles, especially non-isometric shaped, that will rationalize the parameters of operational part in order to reduce the yield of lamellar particles, and, accordingly, to increase the consumer properties of disintegration products.

4. The main part

Figure 1 shows a scheme of centrifugal disintegrator with the blades of both shafts having an outer radius R_1 and accelerating the material in two cylindrical grinding chambers of an inner radius R_2. The material is collected by centrifugal force on periphery of chambers and moves so, that two flows interact on opposite courses along line A_1-B-A_2, coinciding with transverse axis of symmetry of disintegrator. Here material is destroyed by a combination of mutual impact and abrasion of particles from counter flows. At the same time, the maximum intensity of interaction is observed in point B, where the trajectories of blades edges meet with the minimum distance Δ in between.

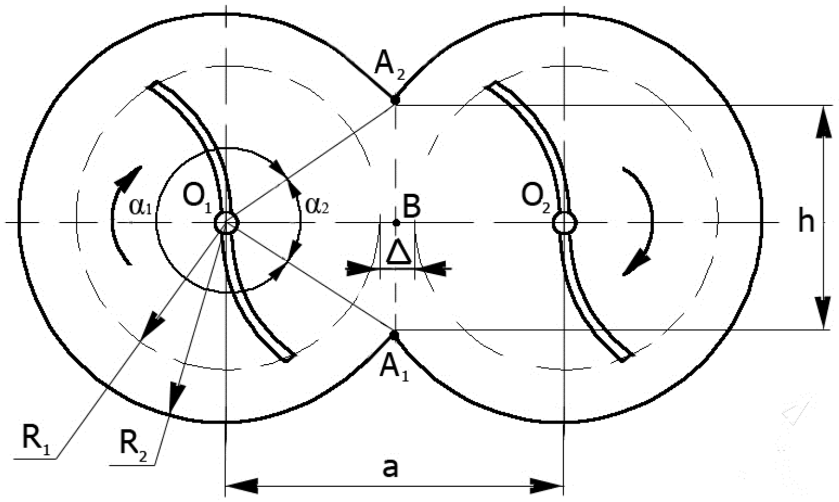

Figure 1. Calculation scheme of counter flow centrifugal disintegrator

The following necessary assumptions are made in order to determine the ratio of energy shares per impact and abrasion of the material:

1) the energy of impact interaction corresponds to the sum of kinetic energies of approaching of the material flows in left and right chambers at points A_1 and A_2, considering that after contact this energy is completely dissipated;

2) the energy of shear deformations at abrasion of particles flows against each other is proportional to sum of works of the particles friction forces in section A_1-B-A_2;

3) the friction force energy during particle movement by circular trajectories along chamber walls is spent on wall wear and represents the loss of disintegration energy;

4) the material is evenly distributed along the height of the grinding chamber (in the direction perpendicular to the plane of figure 1).

The amount of material in the left and the right chambers can be considered being equal to each other. Also, the material motion along A_1-A_2-B-A_1 trajectory in the left chamber is symmetric concerning B point to the motion along A_2-A_1-B-A_2 trajectory in right chamber.

Therefore, we will consider only the left chamber to simplify the problem solving.

4.1. Force balance calculation for the circular section of the loop

In practice, the difference between radius R_1 and radius R_2 is small. Therefore, it is believed, that all the material rotates in the chamber at a constant angular speed ω, in the case of ledges absence on the chamber walls.

The averaged material distribution along the outer boundary of the left chamber (hereinafter referred to as the chamber loop) is shown in Figure 2.

 vol. 27, issue 3 / 2021
pp. 30-39

The amount of material in each small angular sector along the chamber loop is considered equal, bearing in mind the averaging per one turn of the blades. In practice, the rotating blade on the oncoming side will transport an increased amount of material, and after the blade, on the contrary, the amount will be smaller. But this will have just little effect on the total pressure force of the material on the chamber walls along the arc A_1-A_2 in centrifugal field and on the corresponding total friction force. Thus, we will consider the rotation of the material flow regardless of the influence of blades.

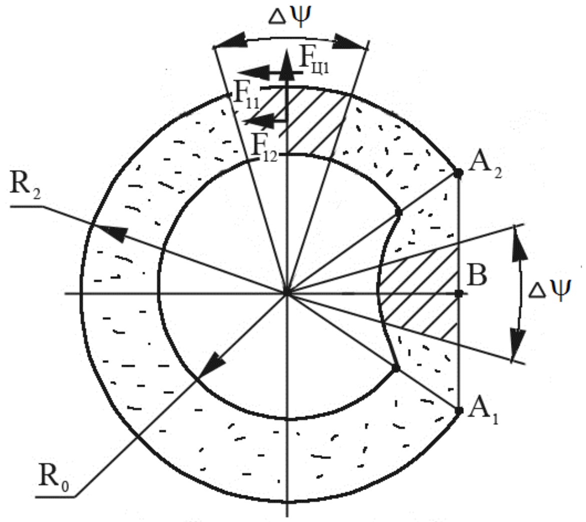

Figure 2. The material distribution and the scheme of friction and inertia forces in the loop circular section

Let's consider the circle arc motion from point A_1 to point A_2.

When moving a small sector of material, a centrifugal force occurs, determined by the formula:

$$\Delta F_{Ц1} = \frac{\gamma}{2}\left(R_2^{\,2} - R_0^{\,2}\right) H \Delta\psi \omega^2 R_c \,, \tag{1}$$

where:

γ is the bulk density of the material;

R_0 is the average radius of inner circle of material loading;

H is the internal height of grinding chamber;

R_c is the average radius of material sector calculated as follows:

$$R_c = \sqrt{\frac{R_2^{\,2} + R_0^{\,2}}{2}} \,. \tag{2}$$

After calculating of the small sector mass

$$\Delta M = \frac{\gamma}{2}\left(R_2^{\,2} - R_0^{\,2}\right) H \Delta\psi \,, \tag{3}$$

we transform the expression (1) as

$$\Delta F_{Ц1} = \Delta M \omega^2 R_c \,. \tag{4}$$

We calculate the filling factor of chamber with material from the expression:

$$\varphi = \frac{\pi\left(R_2^{\,2} - R_0^{\,2}\right)}{R_2^{\,2}\,\frac{\alpha_1 + \sin\alpha_2}{2} - S} \,, \tag{5}$$

where S is the cross-sectional area of the blades and shaft in the plane of Figure 1 (see above), from where we determine the relative filling radius of the chamber:

$$\lambda = \frac{R_0}{R_2} = \sqrt{1 - \varphi\left(\frac{\alpha_1 + \sin\alpha_2}{2\pi} - \frac{S}{\pi R_2^{\,2}}\right)} \,. \tag{6}$$

vol. 27, issue 3 / 2021
pp. 30-39

Total mass of material in one chamber:

$$M_0 = \gamma\pi\left(R_2{}^2 - R_0{}^2\right)H \,. \tag{7}$$

It is also necessary to consider the scheme of normal stresses acting on the material small sector, shown in Figure 3, in order to determine the friction forces of the loose material against the chamber surface.

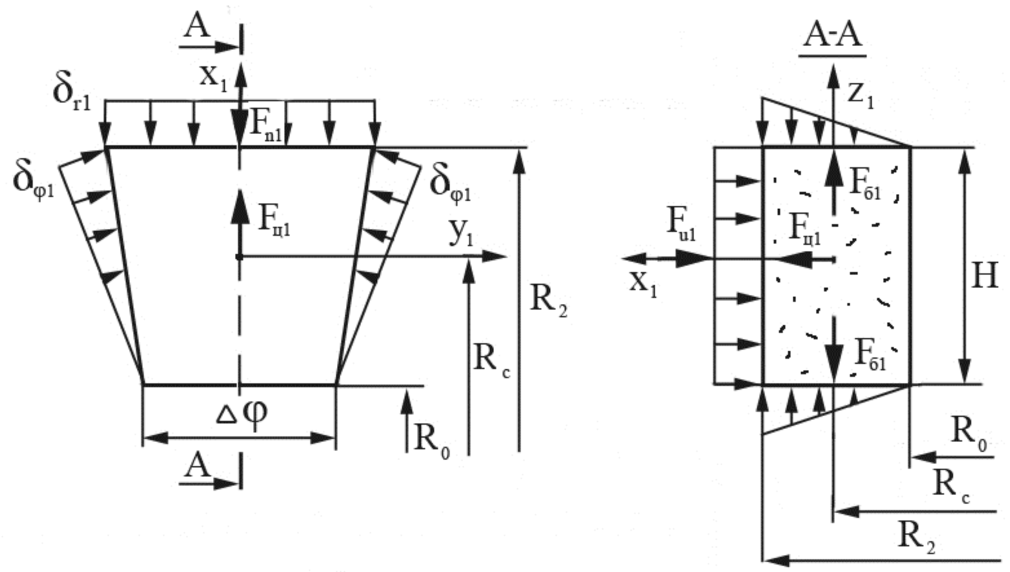

Figure 3. Stress diagrams for the small material sector in the loop circular section

The force balance equation along x1 axis looks so:

$$\sigma_{r1}\Delta\psi R_2 H = \Delta F_{Ц1} + \sigma_{\psi 1}\left(R_2 - R_0\right)H\frac{\Delta\psi}{2} \,, \tag{8}$$

Note here, that the ratio of normal stresses σ_{r1}, σ_{z1} and $\sigma_{\psi 1}$, corresponding to radial, tangential and axial directions, is given by formula

$$\sigma_{\psi 1} = \sigma_{z1} = \xi\sigma_{r1} \,, \tag{9}$$

whereξ is a side thrust coefficient.

After performing some transformations, we calculate:

$$\sigma_{r1} = \gamma\omega^2 R_2{}^2 \frac{\left(1-\lambda^2\right)\sqrt{\dfrac{1+\lambda^2}{2}}}{\left(1-\xi\dfrac{1-\lambda}{2}\right)} = \gamma\omega^2 R_2{}^2 f(\lambda) \,. \tag{10}$$

The normal pressure force on the contact cylindrical part of the sector is calculated from the expression:

$$\Delta F_{n1} = \sigma_{r1} R_2 \Delta\psi H \,, \tag{11}$$

The side thrust force for a small sector of material is determined as follows:

$$\Delta F_{Б1} = \frac{\sigma_{z1}}{4}\left(R_2{}^2 - R_0{}^2\right)\Delta\psi \,, \tag{12}$$

The elementary sliding friction forces when rotating the flow of material in the small sector chamber are calculated as follows:

- against the cylindrical surface:

$$\Delta F_{11} = f_1 \Delta F_{n1} = f_1\gamma\omega^2 R_2{}^3 H\Delta\psi \,; \tag{13}$$

- against the chamber bottom and cover:

$$\Delta F_{12} = 2 f_1 \Delta F_{Б1} = \frac{f_1\xi}{2}\gamma\omega^2 R_2{}^4\left(1-\lambda^2\right)f(\lambda)\Delta\psi \,; \tag{14}$$

where f_1 is the friction coefficient of the material against the chamber surfaces.

Total torque to overcome the friction forces against the chamber surfaces in the circular section of the loop is:

$$T_1 = \left(\frac{\Delta F_{11}}{\Delta \psi} R_2 + \frac{\Delta F_{12}}{\Delta \psi} R_c \right) \alpha_1 = f_1 \gamma \omega^2 \alpha_1 R_2{}^5 \left[\frac{H}{R_2} + \frac{\xi}{2} \left(1 - \lambda^2\right) \sqrt{\frac{1+\lambda^2}{2}} \right] f(\lambda). \tag{15}$$

4.2. Force balance calculation on the rectilinear section of the loop

As mentioned above, the amount of material in each small angular sector for the entire chamber loop is considered to be constant. This means, that the sector of material, based on A_2-A_1 chord, will be convex towards the chamber center (Figure 2, see above). The described increase in the radial thickness of the material layer in the rectilinear section of the loop seems to be reasonable, because the material has increased resistance to movement during friction against the counter flow of the right chamber.

The calculation scheme for the rectilinear section of the loop is shown in Figure 4.

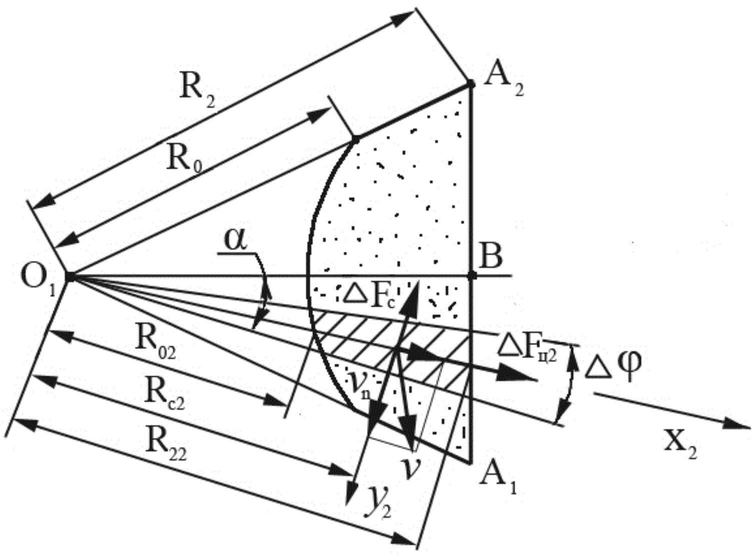

Figure 4. Diagram of inertia and friction forces in the system within the loop rectilinear section

In the diagram, the centrifugal and Coriolis inertia forces act on the considered sector of the material, which center of mass is deviated from O_1-B line by a variable angle α. The mentioned forces are determined by corresponding expressions:

$$\Delta F_{Ц2} = \Delta M \omega^2 R_{c2}\,; \tag{16}$$

$$\Delta F_c = \Delta M\, 2\omega \upsilon_\tau\,, \tag{17}$$

where:

R_{c2} is the variable radius of the center of gravity;

υ_τ is the tangential component of the material speed of movement υ, which is associated with the normal component υ_n by the expression

$$\upsilon_\tau = \upsilon_n \tan\alpha = \omega R_{c2} \tan\alpha\,. \tag{18}$$

Substituting expressions (19) in (17), we obtain:

$$\Delta F_c = \Delta F_{Ц2} \cdot 2\tan\alpha\,. \tag{19}$$

The mass of the material small sector for the loop rectilinear section is approximately calculated as follows:

$$\Delta M_2 = \frac{\gamma}{2}\left(R_{22}{}^2 - R_{02}{}^2\right) H \Delta\psi\,, \tag{20}$$

where:

R_{22} is the variable radius of the material outer border, determined by the formula:

vol. 27, issue 3 / 2021
pp. 30-39

$$R_{22} = R_2 \frac{\cos(\alpha_2/2)}{\cos\alpha}; \tag{21}$$

R_{02} is the variable radius of the material inner border.

Considering the expression (3) together with the previous assumptions will result in the following:

$$R_{02} = \sqrt{R_0^2 + R_2^2 \frac{\cos^2(\alpha_2/2)}{\cos\alpha} - R_2^2}. \tag{22}$$

The variable radius of mass center is as follows:

$$R_{c2} = \sqrt{\frac{R_{22}^2 + R_{02}^2}{2}} = \sqrt{\frac{R_2^2\left(2\frac{\cos^2(\alpha_2/2)}{\cos^2\alpha} - 1\right) + R_0^2}{2}}. \tag{23}$$

Let’s calculate the average radii of material loading on the loop rectilinear section:

- external:

$$R_{22,av} = \frac{1}{\alpha_2}\int_{-\alpha_2/2}^{\alpha_2/2} R_{22}(\alpha)d\alpha; \tag{24}$$

- the radius of gravity center:

$$R_{c2,av} = \frac{1}{\alpha_2}\int_{-\alpha_2/2}^{\alpha_2/2} R_{c2}(\alpha)d\alpha; \tag{25}$$

- internal:

$$R_{02,av} = \frac{1}{\alpha_2}\int_{-\alpha_2/2}^{\alpha_2/2} R_{02}(\alpha)d\alpha. \tag{26}$$

Total inertia forces on the loop rectilinear section:

- centrifugal:

$$F_{Ц2} = \int_{-\alpha_2/2}^{\alpha_2/2} \Delta F_{Ц2}; \tag{27}$$

$$F_{Ц2} = \frac{1-\lambda^2}{2}\gamma\omega^2 R_2^3 R_{c2,av}\frac{H}{R_2}; \tag{28}$$

- Coriolis:

$$F_C = \int_{-\alpha_2/2}^{\alpha_2/2} \Delta F_C = \gamma\omega^2\left(R_2^2 - R_0^2\right)H\int_{-\alpha_2/2}^{\alpha_2/2} R_{c2}(\alpha)\tan\alpha d\alpha = 0. \tag{29}$$

Thus, the Coriolis force accelerates the material along A_2-B section, and symmetrically slowing it down along B-A_1, so its total value in the angular sector is zero.

Let's consider the diagram of normal stresses acting within the loop rectilinear section, shown in figure 5.

We find the total normal force of the material interaction with the counter flow from the equation of force balance along x_2 axis:

$$\sigma_{n2} 2R_2 \sin\frac{\alpha_2}{2}H = F_{Ц2} + 2\frac{\sigma_{\psi1}}{2}(R_2 - R_0)H\sin\frac{\alpha_2}{2}; \tag{30}$$

$$F_{n2} = F_{Ц2} + \sigma_{\psi1}(R_2 - R_0)H\sin\frac{\alpha_2}{2}. \tag{31}$$

The averaged normal stress for A_2-B-A_1 line is calculated as follows:

$$\sigma_{n2} = \frac{F_{n2}}{2R_2\sin\frac{\alpha_2}{2}H}. \tag{32}$$

 vol. 27, issue 3 / 2021
pp. 30-39

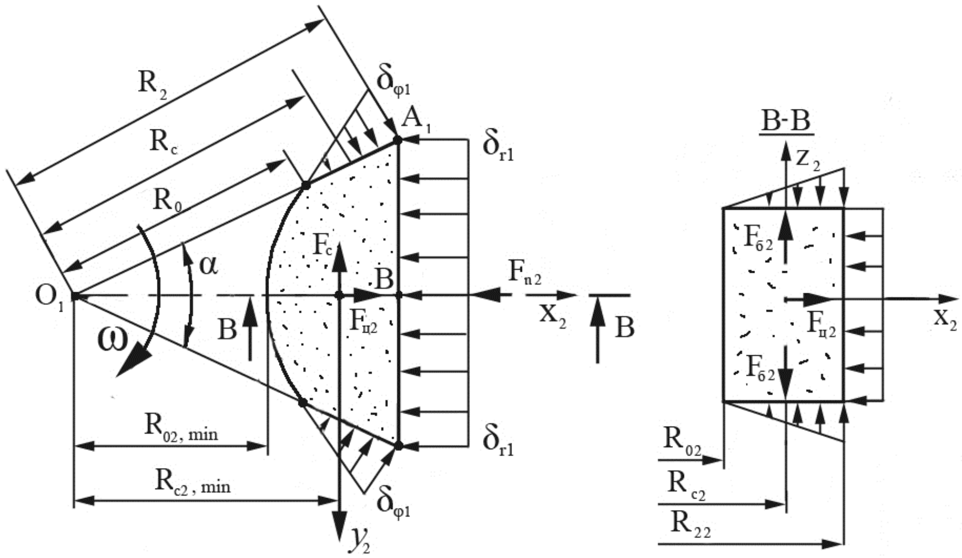

Figure 5. Normal stress diagrams on the loop rectilinear section

The side thrust force for the loop rectilinear section is approximately determined by analogy with equation (12):

$$F_{Б2} \cong \xi \frac{\sigma_{n2}}{4}\left(R_{22,av}{}^2 - R_{02,av}{}^2\right)\alpha_2 \,. \tag{33}$$

Total sliding friction forces during rotation of the material flow in chamber for the loop rectilinear section calculated as follows:

- against counter flow:

$$F_{21} = f_2 F_{n2} \,; \tag{34}$$

- against the chamber bottom and cover:

$$F_{22} = 2 f_1 F_{Б2} \,. \tag{35}$$

where f_2 is coefficient of the material internal friction.

Total torque to overcome friction forces against the opposite material flow is:

$$T_{21} = F_{12} R_2 \cos(\alpha_2/2) . \tag{36}$$

Total torque to overcome friction forces against the chamber on the loop rectilinear section is:

$$T_{22} = F_{22} R_{c2,\min} \,, \tag{37}$$

where $R_{c2,\min}$ is the load minimum internal radius found from expression (23) if $\alpha = 0$:

$$R_{c2,\min} = \sqrt{\frac{R_2{}^2\left(2\cos^2(\alpha_2/2) - 1\right) + R_0{}^2}{2}} \,. \tag{38}$$

4.3. Analysis of the counter flows impact interaction

The material flow in the left chamber, when changing from the loop circular section to the rectilinear section at A_2 point, collides with the flow of the right chamber moving along B-A_2 direction. This is accompanied by a sharp change in the direction of movement at $(\alpha_2/2)$ angle and a hopping drop in the speed of movement.

Let's consider some portion of the material ΔM getting in impact contact with the counter flow.

The kinetic energy of the material portion before impact is calculated as follows:

$$\Delta E_{K,1} = \frac{\Delta M \omega^2 R_c{}^2}{2} \,. \tag{39}$$

The velocity of the material portion mass center immediately after passing the point of A_2, taking into consideration the above assumption of constant angular velocity of flow in any small section of the loop, will be as follows:

 vol. 27, issue 3 / 2021
pp. 30-39

$$\upsilon_{c,2} = \omega R_c \cos\frac{\alpha_2}{2}\ , \tag{40}$$

Then the corresponding kinetic energy after impact is calculated as follows:

$$\Delta E_{K,2} = \frac{\Delta M \omega^2 R_c{}^2}{2}\cos^2\frac{\alpha_2}{2} = \Delta E_{K,1}\cos^2\frac{\alpha_2}{2}\ . \tag{41}$$

We suppose, that the loss of kinetic energy of the flow during passage of A_2 point is completely dissipated to the collision with the opposite flow, which we consider as completely inelastic. The last assumption is quite justified in the presence of several material layers.

Thus, the mechanical work of impact grinding is determined by the formula:

$$\Delta A_{y\partial} = \Delta E_{K,1} - \Delta E_{K,2} = \frac{\Delta M \omega^2 R_c{}^2}{2}\left(1-\cos^2\frac{\alpha_2}{2}\right). \tag{42}$$

All the material in the left chamber passes through A_2 point once per one turn of the flow. Therefore, these calculations can be automatically extended to the entire mass of material in the chamber.

We will find the power in one chamber, consumed for collision with counter flow:

$$N_{y\partial} = \frac{M_0 R_c{}^2 \omega^3}{4\pi}\left(1-\cos^2\frac{\alpha_2}{2}\right). \tag{43}$$

4.4. Analysis of the power structure consumed by the operational part

The power loss during friction of material against the chamber is calculated from the expression:

$$N_{mp} = \left(T_1 + T_{22}\right)\omega\ . \tag{44}$$

The power consumed for destruction of particles by shear deformations at interaction of counter flows:

$$N_{c\partial в} = T_{21}\omega\ . \tag{45}$$

Let us define useful shares of consumed power:

- for impact interaction:

$$\varepsilon_{y\partial} = \frac{N_{y\partial}}{N_{y\partial} + N_{c\partial в} + N_{mp}}\ ; \tag{46}$$

- for shear interaction:

$$\varepsilon_{c\partial в} = \frac{N_{c\partial в}}{N_{y\partial} + N_{c\partial в} + N_{mp}}\ . \tag{47}$$

The last two functions can be represented as functions of key initial parameters:

$$\varepsilon = \chi\left(\varphi, k_S, k_H, \alpha_2, f_1, f_2\right), \tag{48}$$

where:

φ is a technological parameter;

k_S , k_H and α_2 are design parameters;

f_1 and f_2 are parameters responsible for external and internal friction of the material being crushed.

The values of useful shares of the power consumed are not affected by such parameters as γ , ω and R_2 They affect only the absolute value of the power, which is proportional to the density of the material in the first degree, the third degree of the rotation speed of the flow and the fifth degree of the chamber radius.

5. Conclusions and prospects for further development in this direction

The mathematical models of interaction of two counter flows of fine-grained loose material with each other and with surfaces of chambers of centrifugal two-shaft disintegrator are created.

The analytical dependencies of power consumption on impact and shear deformations of fine particles' flows are obtained as functions of the coefficient of chambers filling with material, the design parameters of chamber, as well as the coefficients of internal and external friction of material being crushed.

It has been set, that these shares of power consumption do not depend on the material density, the flow speed and the chamber radius, having other equal dimensionless design parameters.

In contrast, the absolute value of power consumption is directly proportional to the first degree of the material density, the third degree of the flow speed, and the fifth degree of the chamber radius.

These results allow to fulfill further qualitative and quantitative analysis of the influence of each of the six established factors on the values of the consumed power share, to identify the most significant factors and to create a methodology for determining rational parameters of a centrifugal two-shaft disintegrator.

It is also possible to optimize the technological process in order to reduce the yield of lamellar fragments during destruction, which is observed when the proportion of energy of shear deformations increases, in order to obtain cuboid fractions of disintegration products.

References

[1] **Bozhyk, D., Sokur, M., Biletskyi, V., Sokur L.**, 2016
Investigation of the process of crushing solid materials in the centrifugal disintegrators, Easten European Journal of Enterprise Technologies, Vol. 3/7 (81), 2016, pp. 34–41.

[2] **Bozhyk, D.P., Sokur, M.I., Hneushev, V.O., Biletskyi, V.S.**, 2018
Teoretychni i practychni aspekty vyrobnytstva vysokoyakisnoho kubovydnoho shchebeniu (in ukrainian), Visnyk Rivnenskoho natsionalnoho universytetu vodnoho hospodarstva, Tekhnichni nauky, Rivne, 3(79), 2018, pp. 87–95.

[3] **Bozhyk, D.P., Sokur, M.I., Biletskyi, V.S., Yehurnov, O.I., Vorobyov, O.M., Smyrnov, V.O.**, 2017
Pidhotovka korysnykh kopalyn do zbahachennia: Monohrafiia (in ukrainian), Kremenchuk: PP Shcherbatykh O.V., 2017, 392 p.

[4] **Nadutyi, V.P., Lohinova, A.O., Sukhariev, V.V.**, 2017
Udarno-vidtsentrovyi dezintehrator (in ukrainian), Patent Ukrainy na korysnu model 119892, B 02 C 13/14 vid 10.05.2017, opubl. 10.10.2017, Bul. 19.

[5] **x x x**, 2016
DSTU В Б В.2.7-127:2015. Sumishi asfaltobetonni I asfaltobeton shchebenevo-mastykovi. Tekhnichni umovy (in ukrainian), Uved. 01.07.2016, Kyiv: Minregion Ukrainy, 2016, 30 p.

[6] **Lesovik, V.S., Ageeva, M.S., Ivanov, A.V.**, 2011
Nou-khau 20110019. Kompozitsionnoe shlako-tsementnoe viazhushchee dlia proizvodstva melkozernistogo betona (in russian), Ivanov, Federalnoe gosudarstvennoe biudzhetnoe obrazovatelnoe uchrezdenie vysshego professionalnogo obrazovaniya Belgorod. gosud. tekhnol. un-t im. V.G. Shukhova, Data registr. 21.11.2011.

[7] **Sholuyakov, A.D.**, 2017
O proizvodstve vysokokachestvennogo kubovidnogo shchebnia (in russian), Stroitelnyye materialy, 2017, 7, pp. 56–59.

[8] **Lvov, Ye.S.**, 2018
Opredelenie osobennostey dezintegratsii kuskovykh materialov v protsesse drobleniya s ispolzovaniyem dinamicheskikh vozdeystviy (in russian), Gornyy informatsionno-analiticheskiy biulleten, 2018, 11, pp. 154–160, DOI: 10.25018/0236-1493-2018-11-0-154-160.

[9] **Bozhyk, D.P., Sokur, M.I., Biletskyi, V.S., Uchitel, S.O.**, 2017
Teoretychni osnovy kinetyky droblenoho materialu u vidtsentrovo-udarnykh drobarkakh (in ukrainian). Zbahachennia koryshykh kopalyn, naukovo-tekhn. zbirnyk, Dnipro, 68 (109), 2017, pp. 37–45.

[10] **Nadutyi, V.P., Tytov, O.O., Kolosov, D.L., Sukhariev, V.V.**, 2020
Influence of particles geometry on the efficiency of operation of quasistatic and inertial disintegrators (in ukrainian), Naukovyi Visnyk Natsionalnoho Hirnychoho Iniversytetu, (6):021–027, DOI: 10.33271/nvngu/2020-6/021.